

# meso-Tris(oligo-2,5-thienylene)-Substituted Subporphyrins

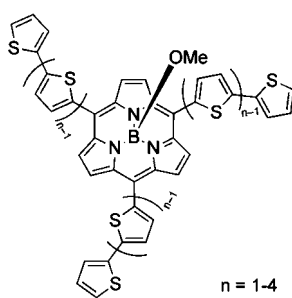
Shin-ya Hayashi, Yasuhide Inokuma, and Atsuhiko Osuka\*

Department of Chemistry, Graduate School of Science, Kyoto University,  
Sakyo-ku, Kyoto 606-8502, Japan

osuka@kuchem.kyoto-u.ac.jp

Received July 27, 2010

## ABSTRACT



**meso-Tris(oligo-2,5-thienylene)-substituted subporphyrins exhibit remarkably red-shifted and intensified absorption bands with increasing number of thienyl subunits. A dimeric subporphyrin obtained from homocoupling of a monobrominated tris(2-thienyl)-substituted subporphyrin exhibits a split Soret-like band due to the exciton coupling.**

Subporphyrin is a genuine ring-contracted porphyrin that was first synthesized as a tribenzosubporphine in 2006.<sup>1</sup> Later, two groups reported the synthesis of *meso*-aryl-substituted subporphyrins independently.<sup>2</sup> Subporphyrins are characterized as a bowl-shaped curved macrocycle, which has 14 $\pi$ -electronic aromatic system and exhibits a porphyrin-like absorption spectrum and intense green fluorescence. An intriguing attribute of subporphyrins is the large influence of *meso*-aryl substituents on the electronic properties of subporphyrins, which leads to the exploration of interesting subporphyrins such as *meso*-oligo(1,4-phenyleneethynylene)-substituted subporphyrins<sup>3a</sup> and *meso*-(4-aminophenyl)-substituted subporphyrins,<sup>3b</sup> both of which exhibit strongly perturbed optical properties.

Recently, we reported the synthesis of *meso*-alkyl-substituted subporphyrins via the reductive desulfurization of *meso*-thienyl-substituted subporphyrins as a key step. During this study, we have noticed that the optical properties of *meso*-thienyl-substituted subporphyrins are considerably perturbed through electronic interaction with *meso*-thienyl substituents.<sup>4</sup> Namely, the Soret bands are red-shifted and broadened, and the fluorescence spectra are red-shifted and enhanced and the Stokes shifts are large, which are larger than those of *meso*-thienyl-substituted porphyrins.<sup>5,6</sup> In

(1) (a) Inokuma, Y.; Kwon, J. H.; Ahn, T. K.; Yoo, M.-C.; Kim, D.; Osuka, A. *Angew. Chem., Int. Ed.* **2006**, *45*, 961–964. (b) Torres, T. *Angew. Chem., Int. Ed.* **2006**, *45*, 2834–2837.

(2) (a) Inokuma, Y.; Yoon, Z. S.; Kim, D.; Osuka, A. *J. Am. Chem. Soc.* **2007**, *129*, 4747–4761. (b) Tsurumaki, E.; Saito, S.; Kim, K. S.; Lim, J. M.; Inokuma, Y.; Kim, D.; Osuka, A. *J. Am. Chem. Soc.* **2008**, *130*, 438–439. (c) Kobayashi, N.; Takeuchi, Y.; Matsuda, A. *Angew. Chem., Int. Ed.* **2007**, *46*, 758–760. (d) Takeuchi, Y.; Matsuda, A.; Kobayashi, N. *J. Am. Chem. Soc.* **2007**, *129*, 8271–8281.

(3) (a) Inokuma, Y.; Easwaramoorthi, S.; Jang, S. Y.; Kim, K. S.; Kim, D.; Osuka, A. *Angew. Chem., Int. Ed.* **2008**, *47*, 4840–4843. (b) Inokuma, Y.; Easwaramoorthi, S.; Yoon, Z. S.; Kim, D.; Osuka, A. *J. Am. Chem. Soc.* **2008**, *130*, 12234–12235.

(4) Hayashi, S.; Inokuma, Y.; Easwaramoorthi, S.; Kim, K. S.; Kim, D.; Osuka, A. *Angew. Chem., Int. Ed.* **2010**, *49*, 321–324.

(5) The bathochromic shift of *meso*-thienylsubporphyrin from *meso*-phenylsubporphyrin in CH<sub>2</sub>Cl<sub>2</sub> is 1430 cm<sup>-1</sup>, while that of porphyrin is small (507 cm<sup>-1</sup>).

(6) *meso*-Thienylporphyrins: (a) Bhyrappa, P.; Bhavana, P. *Chem. Phys. Lett.* **2001**, *349*, 399–404. (b) Gupta, I.; Ravikanth, M. *J. Photochem. Photobiol. A* **2006**, *177*, 156–163. (c) Brückner, C.; Foss, P. C. D.; Sullivan, J. O.; Pelto, R.; Zeller, M.; Birge, R. R.; Crundwell, G. *Phys. Chem. Chem. Phys.* **2006**, *8*, 2402–2412. (d) Santosh, G.; Ravikanth, M. *Chem. Phys. Lett.* **2007**, *448*, 248–252.

particular, the fluorescence quantum yield of *meso*-2-thienyl-substituted subporphyrin is ca. 3-fold larger than that of *meso*-phenyl-substituted subporphyrin, while the opposite trend was reported for the corresponding porphyrins (Figure 1).<sup>6b</sup>

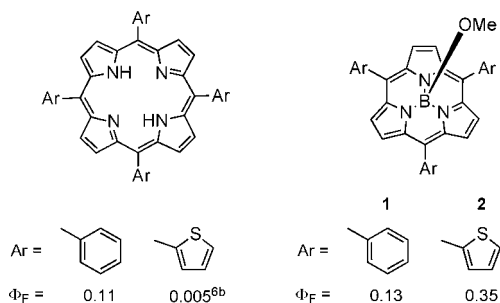
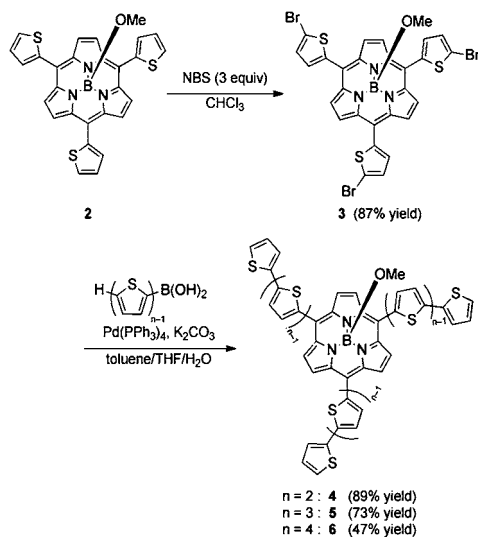


**Figure 1.** Fluorescence quantum yields of *meso*-phenyl and *meso*-thienyl porphyrins and subporphyrins.

With this background, we explored *meso*-oligo(2,5-thienylene)-substituted subporphyrins to see how effectively such substituents influence the optical and electrochemical properties of subporphyrins since oligothiophenes are known to work as semiconductors due to their high mobility under proper conditions.<sup>7</sup> *meso*-Oligo-2,5-thienylene-substituted subporphyrins **4–6** were prepared by Suzuki–Miyaura cross coupling of *meso*-bromothiethylsubporphyrin **3** with the corresponding oligothiophene boronic acids (Scheme 1).

**Scheme 1.** Synthesis of *meso*-Oligothiethylsubporphyrins **4–6**



Subporphyrin **3** was easily prepared by bromination of **2** using 3 equiv of NBS in 87% yield. By following the typical synthetic protocol, subporphyrins **4**, **5**, and **6** were prepared in 89, 73, and 47% yields, respectively, while longer reaction time and higher temperature were needed

for the synthesis of **6**. Attempts to further elongate the thienylene chain failed because of the serious solubility problem. The high-resolution electrospray ionization (HR-ESI) mass spectra of **4–6** revealed intense boronium cation peaks at  $m/z$  734.0148 (calcd for  $C_{39}H_{21}B_1N_3S_6 = 734.0154$  [**4-OMe**]<sup>+</sup>),  $m/z$  979.9790 (calcd for  $C_{51}H_{27}B_1N_3S_9 = 979.9788$  [**5-OMe**]<sup>+</sup>), and  $m/z$  1225.9390 (calcd for  $C_{63}H_{33}B_1N_3S_{12} = 1225.9421$  [**6-OMe**]<sup>+</sup>), respectively.

The structures of subporphyrins **4** and **5** were unambiguously confirmed by single-crystal X-ray diffraction analyses (Figure 2). In both cases, the subporphyrin cores show bent

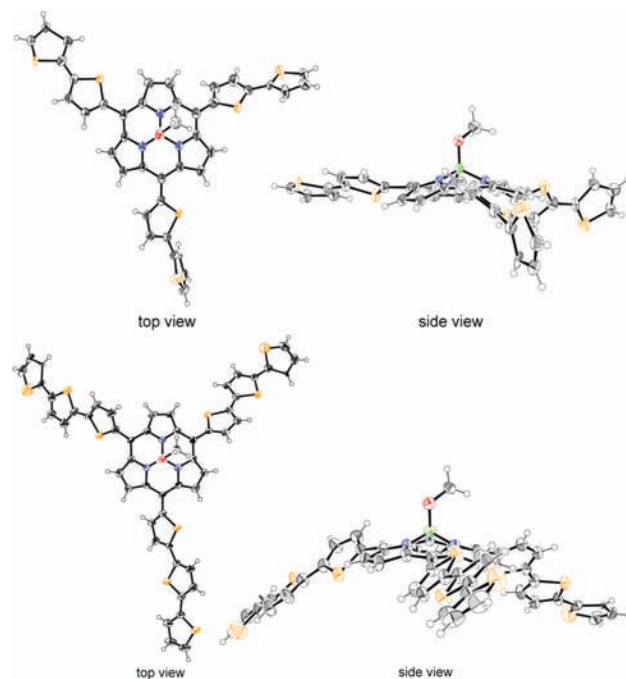


**Figure 2.** X-ray crystal structures of **4** (top) and **5** (bottom). Thermal ellipsoids are set at the 50% probability level.

bowl-shaped structures and the mean dihedral angles of the thienyl substituents toward the subporphyrin core are rather small, being 35.9 and 41.5°, respectively, as compared with those of *meso*-aryl-substituted subporphyrins. Interestingly, the oligothiophylene segments are aligned in a roughly planar manner in the solid state, which is favorable for  $\pi$ -conjugation.

Figure 3 shows the UV/vis absorption and fluorescence spectra of **2**, **4**, **5**, and **6**. With increasing number of thienylene subunits, the Soret-like bands are red-shifted and intensified continuously with peak positions of 394, 420, 436, and 446 nm, while the Q-like bands were observed in the same manner at 522, 557, 572, and 575 nm, respectively. Along these changes, the fluorescence spectra are also red-

(7) (a) *Electronic Materials: The Oligomer Approach*; Müllen, K., Wegner, G., Eds.; VCH: Weinheim, Germany, 1998; pp 105–197. (b) Zhang, F.; Bäuerle, P. *J. Am. Chem. Soc.* **2007**, *129*, 3090–3091. (c) Izumi, T.; Kobashi, S.; Takimiya, K.; Aso, Y.; Otsubo, T. *J. Am. Chem. Soc.* **2003**, *125*, 5286–5287.

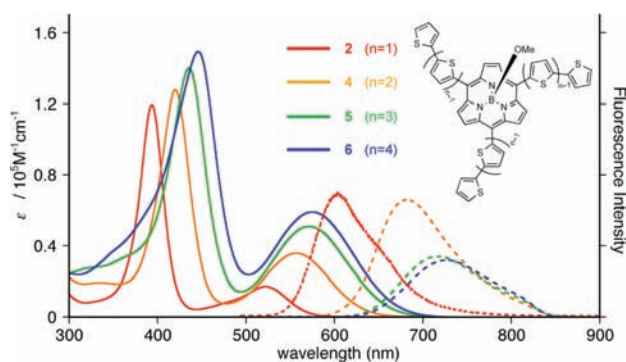


**Figure 3.** UV/vis absorption (solid lines) and fluorescence (dashed lines) spectra of **2**, **4**, **5**, and **6** in  $\text{CH}_2\text{Cl}_2$ .

shifted with peak positions of 603, 680, 714, and 727 nm, respectively. These spectral changes reveal the effective electronic interactions between the subporphyrin core and *meso*-oligothienylene chains. Interestingly, the fluorescence quantum yields are high for **2** ( $\Phi_F = 0.35$ ) and **4** ( $\Phi_F = 0.33$ ) but are dropped for **5** ( $\Phi_F = 0.17$ ) and **6** ( $\Phi_F = 0.16$ ). Here, it is worth noting that the optical properties of **5** and **6** are rather similar, suggesting a saturation feature for oligoethienylene conjugation. In order to examine these substituent effects, we have performed DFT calculations. Molecular structures of **2** and **4–6** were optimized at the B3LYP/6-311G(d) level using the Gaussian 09 package,<sup>8</sup> and MO diagrams were calculated as shown in Figure S6-1 (see Supporting Information). Subporphyrin **2** has  $a_{2u}$ -like HOMO and  $a_{1u}$ -like HOMO-1. HOMOs of **4–6** are similar to **2**, showing the electronic coefficients on both the pyrrole and *meso*-thienylene units. Importantly, the coefficients of HOMO are spread up to the third thienylene subunit but are merely marginal on the fourth one in **6**. On the other hand, the  $a_{1u}$ -like orbitals of **2** and **4–6** are not strongly perturbed. Degenerate LUMOs are stabilized along with elongation of thienylene subunits but show similar saturation behaviors around the third or fourth subunit, in line with the experimental observations. As judged from the spectral changes and MO calculations of subporphyrins, it is concluded that the influences of *meso*-oligo(2,5-thienylene) substituents are stronger than those of *meso*-oligo(1,4-phenyleneethynylene) substituents.<sup>3a</sup>

The oxidation and reduction potentials of the subporphyrins were measured by cyclic voltammetry in  $\text{CH}_2\text{Cl}_2$  containing 0.10 M  $\text{Bu}_4\text{NPF}_6$  as a supporting electrolyte. (Figure 4). *meso*-Thienylsubporphyrin **2** exhibited a reversible oxidation potential at 0.68 V and a reversible reduction potential at  $-1.74$  V. *meso*-Oligo(2,5-thienylene)-substituted subporphyrins **4–6** show two reversible reduction potentials, which decrease with increasing number of thienylene units.

In addition, to demonstrate the synthetic utility of these *meso*-thienylene-substituted subporphyrins, bithiophene-bridged subporphyrin dimer **8** was prepared by a Ni-catalyzed

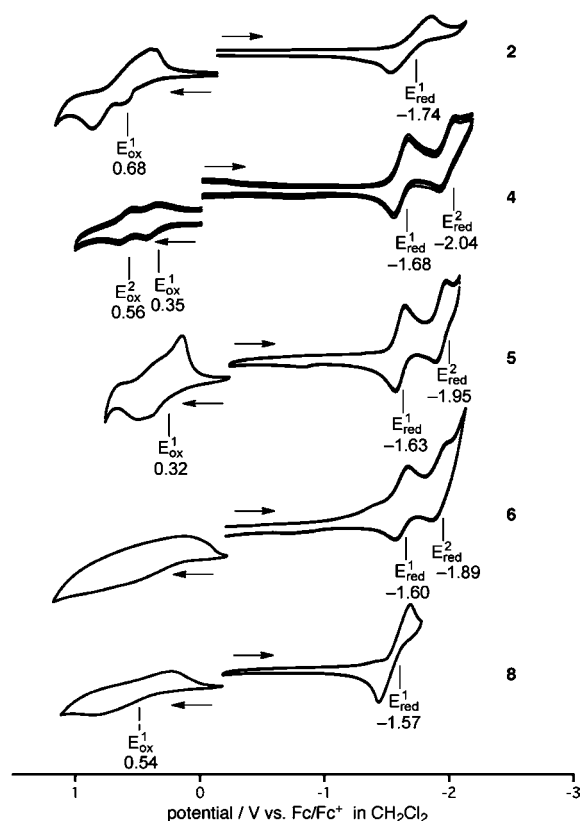
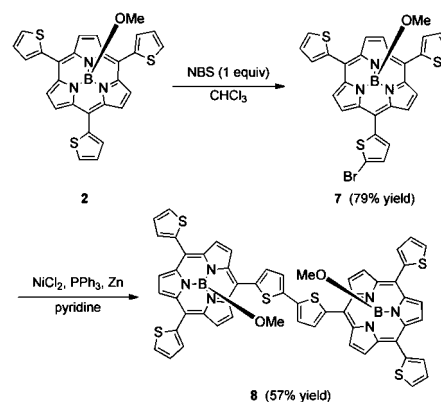


**Figure 4.** Cyclic voltammograms of **2**, **4–6**, and **8**.  $\text{Fc}/\text{Fc}^+$  = ferrocene/ferrocenium.

Negishi coupling reaction<sup>9</sup> of monobromothieryl-substituted subporphyrin **7**, which was prepared by careful bromination of **2** with an equivalent of NBS in 79% yield (Scheme 2). A

#### Scheme 2. Synthesis of Bithiophene-Linked Dimer **8**



pyridine solution of **7** was refluxed in the presence of  $\text{NiCl}_2$ , triphenylphosphine, and zinc dust for 1 h to provide **8** in 57% yield. The HR-ESI mass spectrum of **8** revealed an

(8) For the full citation, see the Supporting Information.

(9) Tao, X.-C.; Zhou, W.; Zhang, Y.-P.; Dai, C.-Y.; Shen, D.; Huang, M. *Chin. J. Chem.* **2006**, *24*, 939–942.

intense boronium cation peak at  $m/z$  1005.1056 (calcd for  $C_{55}H_{31}B_2N_6O_1S_6 = 1005.1081$  [ $\mathbf{8}\text{-OMe}$ ] $^+$ ). The  $^1\text{H}$  NMR spectrum supported the assigned dimeric structure by displaying a singlet at  $\delta = 8.33$  ppm, a couple of doublets at  $\delta = 8.43$  and  $8.36$  ppm due to the  $\beta$ -protons, three sets of signals due to the protons of the outer thiophenes, two sets of signals due to the protons of the inner thiophenes, and a singlet signal of the axial methoxy protons.

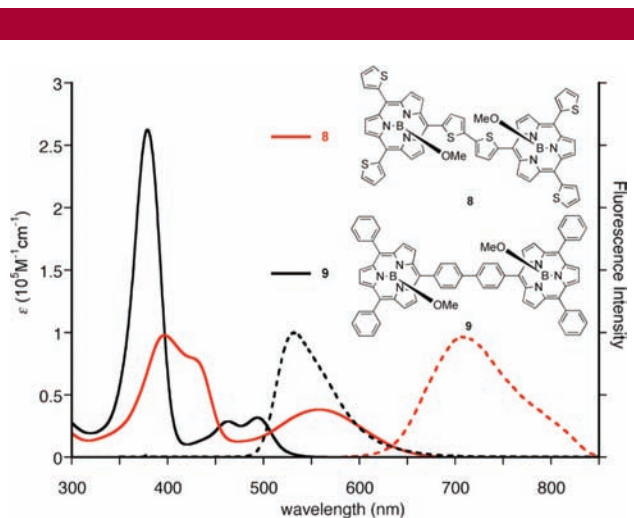


**Figure 5.** UV/vis absorption (solid lines) and fluorescence (dashed lines) spectra of subporphyrin dimers **8** and **9** in  $\text{CH}_2\text{Cl}_2$ .

Figure 5 displays the UV/vis absorption and fluorescence spectra of dimer **8** in  $\text{CH}_2\text{Cl}_2$  along with those of 4,4'-biphenylene-bridged subporphyrin dimer **9** since **9** shows through-bond interactions through a 4,4'-biphenylene bridge, which was not observed for the corresponding porphyrin dimer.<sup>10</sup> It is obvious that the absorption and emission bands of **8** are much broader and extensively red-shifted compared with those of **4** and **9**. It is remarkable that the Q-like band and the fluorescence of **8** are observed at 559 and 708 nm, respectively. More importantly, the dimer **8** displays a

(10) Inokuma, Y.; Osuka, A. *Org. Lett.* **2008**, *10*, 5561–5564.

distinctly split Soret band at 397 and 425 (sh) nm, probably due to the exciton coupling of the two subporphyrin chromophores. It is worthy to note that **8** is the first subporphyrin dimer exhibiting a split Soret-like band, and such strong electronic interaction was not observed for the corresponding bithiophene-bridged porphyrin dimer.<sup>11</sup> As another interesting feature, the dimer **8** has a significantly larger Stokes shift ( $3764\text{ cm}^{-1}$ ) than that of *meso*-thienyl-subporphyrin **2** ( $2573\text{ cm}^{-1}$ ), suggesting large structural changes in the excited state of dimer **8**. Electrochemical potentials for **8** were measured by CV experiment, in which reversible reduction and oxidation waves were observed at  $-1.57$  and  $0.54$  V in  $\text{CH}_2\text{Cl}_2$ , respectively (Figure 4). The strong electronic interaction in **8** can be understood in terms of its MO feature, in which large orbital coefficients are found not only at the subporphyrin cores but also at the bithiophene bridge (see Supporting Information).

In summary, we have synthesized *meso*-oligo-2,5-thienylene-substituted subporphyrins and revealed their effective conjugative interactions. Synthetic utility of these subporphyrins has been demonstrated by the preparation of a bithiophene-bridged subporphyrin dimer, which shows even more effective  $\pi$ -conjugation through the bridge. Along this line, we are currently exploring larger dendritic bithiophene-bridged subporphyrin systems.

**Acknowledgment.** This work was supported by the Global COE Program “International Center for Integrated Research and Advanced Education in Materials Science” (No.B-024) and Grants-in-Aid (Nos. 22245006 (A) and 20108001 “ $\pi$ -Space”) for Scientific Research from MEXT. Y.I. thanks the JSPS Research Fellowship for Young Scientists.

**Supporting Information Available:** Experimental details and characterization of new compounds and crystal data. This material is available free of charge via the Internet at <http://pubs.acs.org>.

OL101746D

(11) Odobel, F.; Suresh, S.; Blart, E.; Nicolas, Y.; Quintard, J.-P.; Janvier, P.; Le Questel, J.-Y.; Illien, B.; Rondeau, D.; Richomme, P.; Häupl, T.; Wallin, S.; Hammarström, L. *Chem.—Eur. J.* **2002**, *8*, 3027–3046.